

**NIST Technical Note 1928**

# **The Structure of a Moderate-Scale Methanol Pool Fire**

Anthony Hamins  
Andrew Lock

This publication is available free of charge from:  
<https://doi.org/10.6028/NIST.TN.1928>

**NIST**  
**National Institute of  
Standards and Technology**  
U.S. Department of Commerce

**NIST Technical Note 1928**

# **The Structure of a Moderate-Scale Methanol Pool Fire**

Anthony Hamins  
*Fire Research Division  
Engineering Laboratory*

Andrew Lock  
*Office of Hazard Identification and Reduction  
U.S. Consumer Product Safety Commission  
Rockville, MD 20850*

This publication is available free of charge from:  
<https://doi.org/10.6028/NIST.TN.1928>

November 2016



U.S. Department of Commerce  
*Penny Pritzker, Secretary*

National Institute of Standards and Technology  
*Willie May, Under Secretary of Commerce for Standards and Technology and Director*

Certain commercial entities, equipment, or materials may be identified in this document in order to describe an experimental procedure or concept adequately. Such identification is not intended to imply recommendation or endorsement by the National Institute of Standards and Technology, nor is it intended to imply that the entities, materials, or equipment are necessarily the best available for the purpose.

**National Institute of Standards and Technology Technical Note 1928  
Natl. Inst. Stand. Technol. Tech. Note 1928, 11 pages (November 2016)  
CODEN: NTNOEF**

**This publication is available free of charge from:  
<https://doi.org/10.6028/NIST.TN.1928>**

## Table of Contents

Abstract.....	ii
1. Introduction.....	1
2. Experimental Method.....	2
2.1 Pool Burner .....	2
2.2 Temperature Measurement.....	3
2.3 Gas Species Measurement.....	4
3. Results and Discussion .....	5
3.1 Temperature Measurements .....	6
3.2 Species Concentrations.....	8
3.3 Radiative Distribution .....	9
4. Conclusions.....	10
5. References.....	11

## Temperature and Species Measurements in a Moderate-Scale Methanol Pool Fire

### ABSTRACT

A series of measurements was made to characterize the structure of a moderate-sized methanol pool fire steadily burning in a quiescent environment. Time averaged local measurements of temperature and gas species concentrations were made in a steadily burning methyl alcohol (methanol; CH<sub>3</sub>OH) pool fire. Temperatures were measured using fine wire thermocouples corrected for radiative losses. Gaseous species were measured using extractive sampling through a cooled probe and the samples analyzed using a gas chromatograph. The species measured included the reactants (the fuel, methanol, and oxygen), combustion intermediates such as CO and combustion products such as H<sub>2</sub>O and CO<sub>2</sub>. It is anticipated that these data will be useful for model validation.\*

**KEYWORDS:** burning rate, gas species, methanol, pool fires, temperature

---

\* Certain commercial products are identified in this report in order to specify adequately the equipment used. Such identification does not imply recommendation by the National Institute of Standards and Technology, nor does it imply that this equipment is the best available for the purpose.

## 1. INTRODUCTION

The focus of this report is on the structure of a moderate-scale liquid methanol pool fire steadily burning in a well-ventilated quiescent environment. Pool fires are a fundamental type of combustion phenomena in which the fuel surface is flat and horizontal, which provides a simple and well-defined configuration to test models and further the understanding of fire phenomena. For liquid pool fires, the boundary condition at the pool surface obeys the Clausius-Clapeyron relation with the surface isothermal and observed to be approximately at the boiling point. In this study, methanol is selected as the fuel. Fires established using methanol are unusual as no carbonaceous soot is present or emitted. This creates a particularly useful testbed for fire models and their radiation submodels that consider emission by gaseous species - without the confounding effects of blackbody radiation from soot.

Use of fire modeling in fire protection engineering has increased dramatically during the last decade due to the development of practical computational fluid dynamics fire models and the decreased cost of computational power. Today, fire protection engineers use models like the Consolidated Fire and Smoke Transport Model (CFAST) and the Fire Dynamics Simulator (FDS) to design safer buildings, nuclear power plants, aircraft cabins, trains, and marine vessels to name a few types of applications. [1, 2] To be reliable, the models require validation, which involves a large collection of experimental measurements. An objective of this report is to provide data for use in fire model evaluation by the fire research community.

In moderate and large-scale pool fires, radiative heat transfer is the dominant mechanism of heat feedback to the fuel surface. Species concentrations and temperatures have a large influence on the radiative heat transfer. A zone of particular interest is the fuel rich-core between the flame and the pool surface, where gas species can absorb energy that would otherwise have been transferred to the fuel surface.

In this study, previous measurements characterizing the structure of a moderate-sized methanol pool fire are presented including time averaged local temperature and gas species concentrations. Temperatures were measured using fine wire thermocouples corrected for radiative losses. Gaseous species were measured using extractive sampling and a gas chromatograph. The species measured included the reactants (the fuel, methanol, and oxygen), combustion intermediates such as  $H_2$  and  $CO$ , and combustion products such as  $H_2O$  and  $CO_2$ . The measurement results reported here represent experiments that were conducted during the years 2006 to 2008 at the National Institute of Standards and Technology (NIST). Some previously reported results are shown here for completeness – as this information is needed to define the fires for modeling purposes. Reference to previous work is made as appropriate.

The methanol pool fire considered in this study has been previously investigated. Akita and Yumoto [3] and Hamins et al [4] used ring pool burners to investigate the mass burning rate as a function of distance from the pool center. Weckman and Strong made measurements of the velocity and temperature fields up to one diameter above the fuel surface of a methanol pool fire for conditions very similar to those considered here – they used a 30.5 cm diameter burner with a rim height of 1 cm. [5] Radiative heat flux distribution to the fuel surface and to the surroundings are discussed in Refs. [4, 6, 7]. Global flame parameters such as the mean flame height and pool fire pulsation frequency have also been characterized [5, 7]. Ref. [8] used computational fluid dynamic fire modeling to examine 30 cm methanol pool fires.

Table 1 provides a list of previous measurements in a (nominally) 30 cm diameter methanol pool fire. These previous studies are complementary to the measurements reported here.

Table 1. Parameters Measured in Well-Ventilated Steadily Burning Nominally 30 cm Diameter Methanol Pool Fires.

Parameter	Reference
Mean flame height	7
Pulsation frequency	5
Radiative fraction	6, 7
Mass loss rate	3, 4, 5, 9
Energy Balance	4
Radiative flux distribution onto fuel surface	4
Radiative flux distribution to the surroundings	6, 7, 9
Vertical temperature distribution in the fuel	4
Gas species volume fraction	this study, 10
Temperature Field	this study, 5
Velocity Field	5

This report is broken into several parts. In Section 2, the experimental method and apparatus are described. The results are summarized in Section 3 and references are provided in Section 4.

## 2. EXPERIMENTAL METHOD

Steady-state burning conditions were established before measurements were initiated. A warm-up period of about 10 min was required for the mass burning rate to be steady. Since back diffusion of water slowly accumulates in the fuel pool in methanol fires, fresh fuel was used between experiments. Experiments were conducted under an exhaust hood located 2 m above the burner rim. The pool burner was situated in an enclosure (2 m by 2 m) built of double mesh screen walls to reduce the effect of ambient convective currents on the fire. The experimental apparatus and methods have been previously described in some detail in Refs. [4, 7, 11].

### 2.1 Pool Burner

A circular stainless steel pan with an outer diameter ( $D$ ) of 0.30 m, a depth of 0.15 m, and a wall thickness of 0.0016 m held the liquid methanol. An image of the burner is seen in Figure 1. The bottom of the burner was water cooled with water (16 °C) flowing through a coiled copper tube brazed to the bottom of the fuel pan, which kept the bottom of the burner at a constant temperature. The burner was mounted on “legs” such that burner rim was about 0.4 m above the ground. A fuel overflow basin included for safety extended 3 cm beyond the burner wall at its base.

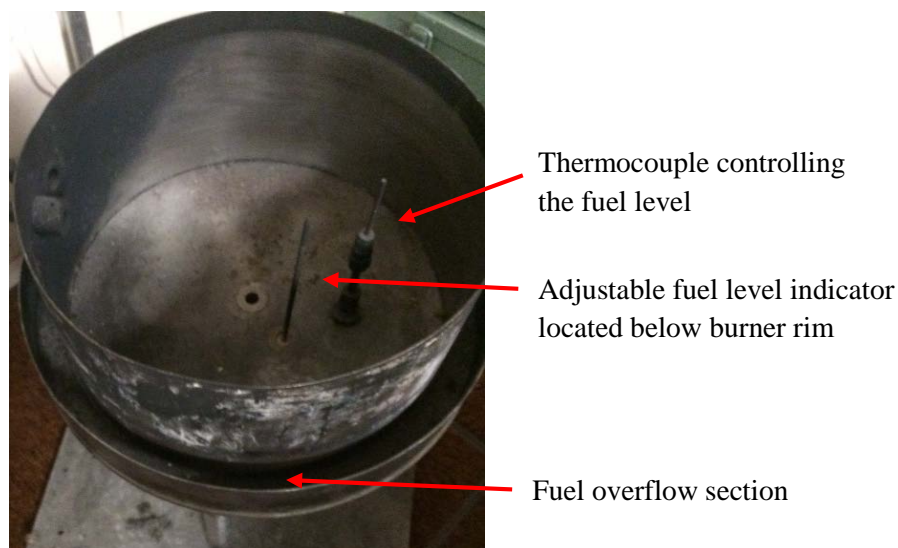


Figure 1. The 30 cm burner with fuel level indicator and fuel overflow section.

Fuel to the burner was gravity fed from a reservoir on a mass load cell monitored by a data acquisition system. The fuel level in the burner has an impact on the mass burning rate. [4] During these experiments, the level of the fuel was maintained 5 mm below the burner rim by regulating the fuel supply from the reservoir to the burner. An off-center hole on the bottom of the burner held a stainless-steel sheathed thin ( $\approx 1.6$  mm diameter) Type K (chromel-alumel) thermocouple which measured the temperature just above the surface of the pool at the plane defined by the burner rim. During a fire, vaporization of the fuel caused the liquid level to drop and the thermocouple temperature to rise. The rising temperature triggered a control signal to the fuel flow control valve, allowing additional fuel to flow into the burner, facilitating maintenance of the liquid at a near constant level in the burner. The liquid set-point temperature determines the fuel level. It was set a few degrees above the fuel boiling point of  $65$  °C. The level was verified throughout the experiment by visually observing the tiny tip of a sharpened (2 mm diameter) pointer that formed a barely discernable dimple on the fuel surface. The fuel level indicator is seen near the center of the burner in Figure 1. The expanded uncertainty in the level was estimated to be 0.5 mm for the methanol experiments.

## 2.2 Temperature Measurement

A bare-bead thermocouple situated in a fire experiences radiative exchange with the flames and the surrounding environment such that the measured temperature is not the true gas temperature. In this study, the local temperature was measured using fine wire thermocouples. A computer controlled translation stage moved the thermocouple through the flame. The flame was assumed to be axisymmetric.

The thinner the wires, the smaller the radiative loss and the faster the measurement time response. Selection of the diameter of a fine wire thermocouple must consider trade-offs between the durability of the instrument and measurement needs. The finer the wire, the smaller the radiative exchange with the environment, but the more difficult it is to configure. In this study, a  $75$   $\mu\text{m}$  diameter Type S (Pt 10% Rh/Pt) thermocouple was employed. The measured signal was acquired at a rate of 10 Hz for at least 30 flame cycles. The signal was recorded and the time-average and standard deviation calculated.



Temperature measurements were corrected for radiative losses considering an energy balance at the thermocouple bead. No soot was present in the methanol fire, so the thermocouple geometry remained invariant with time. The bead was approximately spherical as seen in an optical microscope with the bead diameter approximately two times the diameter of the lead wires. The thermocouple leads were oriented horizontally in the fire, so conductivity along the leads was assumed to be negligible. The convective-radiative energy balance can be written as:

$$(T - T_m) Nu k / D = \sigma \varepsilon (T_m^4 - T_a^4) \quad (1)$$

where  $T$  is the gas temperature,  $T_m$  is the temperature at the thermocouple bead,  $T_a$  is the ambient temperature (298 K),  $k$  is the gas thermal conductivity,  $D$  is the diameter of the thermocouple bead,  $\sigma$  is the Stefan–Boltzmann constant,  $\varepsilon$  is the thermocouple emissivity, and  $Nu$  is the Nusselt number. The Nusselt number for a sphere is given by Ref. [12]:

$$Nu = 2 + (0.4 Re^{1/2} + 0.06 Re^{2/3}) Pr^{2/5} (\mu/\mu_s)^{1/4} \quad (2)$$

where  $Re$  is the Reynolds number,  $Pr$  is the Prandtl number,  $\mu$  is the gas viscosity and the subscript “s” refers to conditions on the thermocouple surface. The temperature dependent gas properties for  $k$ ,  $\mu$ ,  $Re$ ,  $Pr$ , are taken as those of air from Ref. [12], which also provides the emissivity of platinum at elevated temperatures. Solving Eq. 1 for  $T$ , a radiative correction for the gas temperature was found to be less than 30 K for the peak temperature. To determine the  $Re$ , the measured gas velocity in a 30.5 cm methanol fire was taken from Ref [5], but the sensitivity to velocity is very small. The total expanded uncertainty in the temperature measurement was determined to be 16 %, which was almost entirely due to measurement variance.

### 2.3 Gas Species Measurement

The volume fractions of major gas species were measured along the centerline of the pool fire using an Agilent 3000A Micro-GC gas chromatograph fitted with thermal conductivity detectors (TCD) detectors. Species samples were extracted using a cooled probe at various locations along the fire centerline during steady-state burning.

The GC was able to quantify a number of stable reactants, intermediates, and combustion product species extracted from the fire during each test. Chromatographic separation of species was achieved by four columns working in parallel, namely a molecular sieve 5A, Plot-U, OV-1, and Stabilewax columns. Helium was used as carrier gas on all of the columns except the mole-sieve column, for which Argon was used. A summary of the different columns, their physical specifications, and the GC parameters used during the analysis are listed in Table 2.2 of Ref. [13].

A cooled probe connected to a gas pump extracted samples from the flame. The probe was composed of two concentric stainless steel tubes with an outer annular coolant flow and an inner extracted gas sample flow. The inner and outer tube diameters were 4.5 mm and 12.7 mm, respectively. Dimethyl-phenylmethylsiloxane was used as the coolant. It was preheated to 100 °C to prevent condensation of H<sub>2</sub>O and methanol in the probe during sampling. The remainder of the sampling line to the GC was heated with electrical heating tape at 100 °C. Gas samples were drawn through the inner tube at a rate of

30 cm<sup>3</sup>/s into heated gas lines and a 300 cm<sup>3</sup> heated glass mixing vessel, where the residence time was about 9 s. Sample was injected into the GC from the mixing vessel.

Identification and quantification of gaseous species was accomplished by the use of gas phase calibration standards either commercially purchased or mixed in the lab. Liquid calibration mixtures involving H<sub>2</sub>O and CH<sub>3</sub>OH, for example, were created in the lab and introduced into the GC using a special injection port. Due to the wide variety of columns used and the large number of species and varying quantities that were potentially present, several different gas standards were used.

Uncertainty in the quantification of gas species is described in detail in Ref. [13]. Typically, a minimum of 4 or 5 samples were analyzed at each location. The variance in the measurement results differed from location to location and from species to species. On average, for all species, the repeatability or variance of the measurement was 16 %, which was the single most important component in the overall uncertainty budget. The expanded uncertainty was 34 %, on average, for all gas species.

### 3. RESULTS AND DISCUSSION

The shape of the fire dramatically changed during its pulsing cycle. The fire was blue with no indication of the presence of soot. The observed dynamic fire shape is consistent with the careful description given by Weckman and Sobiesiak for a medium-scale acetone pool fire [14] and with the analysis given by Baum and McCaffrey [15].

Figure 2 shows two images of the pulsing methanol pool fire burning in the 0.30 m stainless-steel water-cooled burner. A series of repeated cycles in which orderly curved flame sheets anchored at the burner rim and connected to the central fire plume roll towards the fire centerline and neck-in to form a narrow and long visible fire plume.

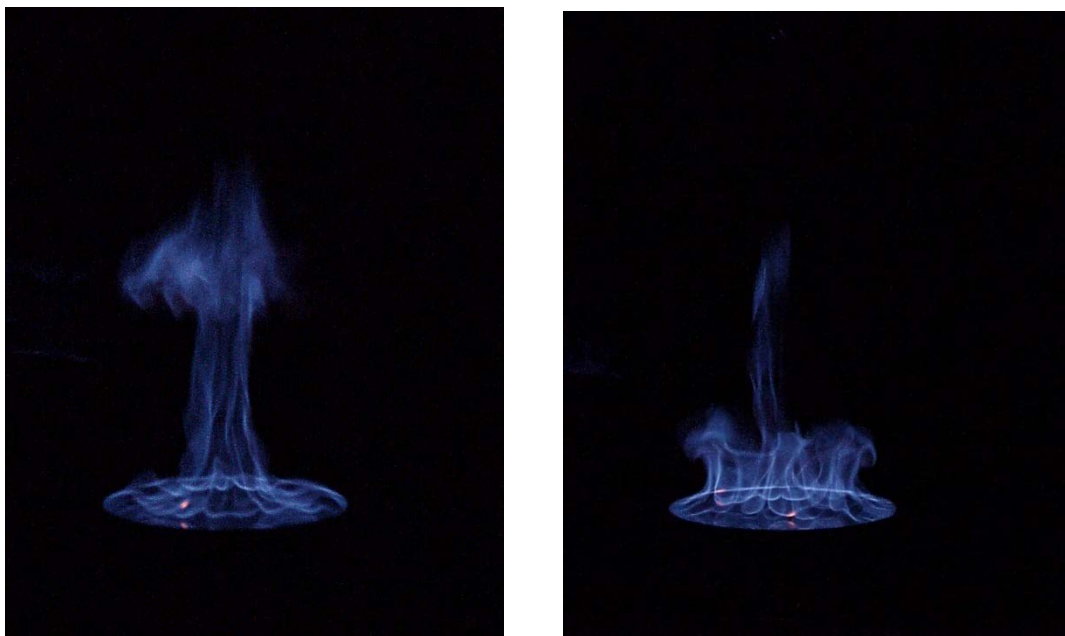


Figure 2. Instantaneous digital images of the pulsing 0.30 m diameter methanol pool fire.

### 3.1 Temperature Measurements

The time-averaged temperature measurements as a function of distance above the burner along the centerline are shown in Figure 3. The maximum temperature was 1323 K, which occurred about 15 cm above the fuel surface at a flame location where much of the fuel has reacted and near the maximas of the concentrations of intermediate gas species such as CO and H<sub>2</sub> (see the results and discussion in Section 3.2 below). Also shown are temperature measurements from Weckman and Strong in their 30.5 cm diameter methanol pool fire with a rim height of 1 cm [5]. They used bare 50  $\mu$ m diameter Type S (Pt 10% Rh/Pt) wire thermocouples, similar to the thermocouples used in this study. Representative values of the expanded uncertainty, which was dominated by measurement variance, are shown in the figure. A comparison of the results seen in Figure 3 show that the data are in general agreement.

The gradient near the fuel surface in Fig. 2 is steep. At a location 0.3 cm above the burner rim, which is 0.8 cm above the fuel surface, the temperature was about 730 K, whereas the temperature at the fuel surface was measured to be at the boiling point of methanol, 338 K, yielding a temperature gradient near the fuel surface of about 500 K/cm.

Figure 4 shows analogous results for radial radiation-corrected temperature profiles at various axial distances above the burner in a 0.30 methanol pool fire. Results from Weckman and Sobesiak at 30 cm above the burner are shown for comparison [14]. Representative values of the expanded uncertainty, which was dominated by measurement variance, which were previously not presented, are shown in the figure. The largest temperatures in the radial direction occur on or close to the central axis.

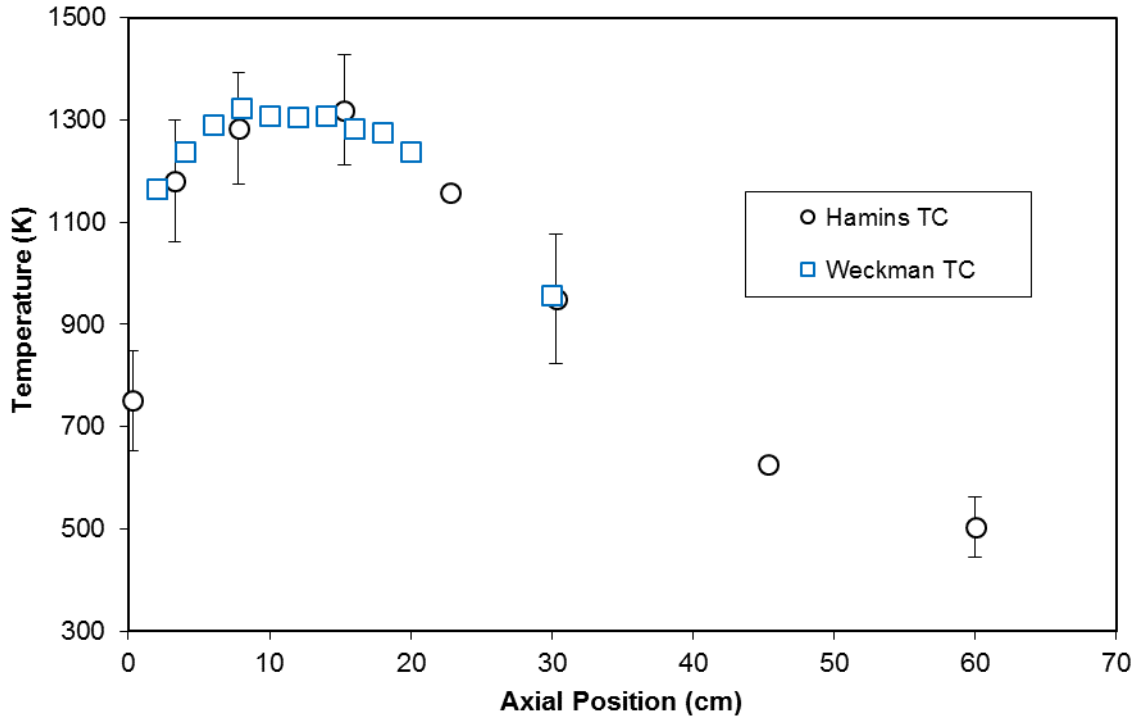


Figure 3. Fine-wire radiation-corrected thermocouple temperature profiles as a function of distance above the burner along the centerline of a 0.30 methanol pool fire. Results from Weckman and Strong are also shown. [5]

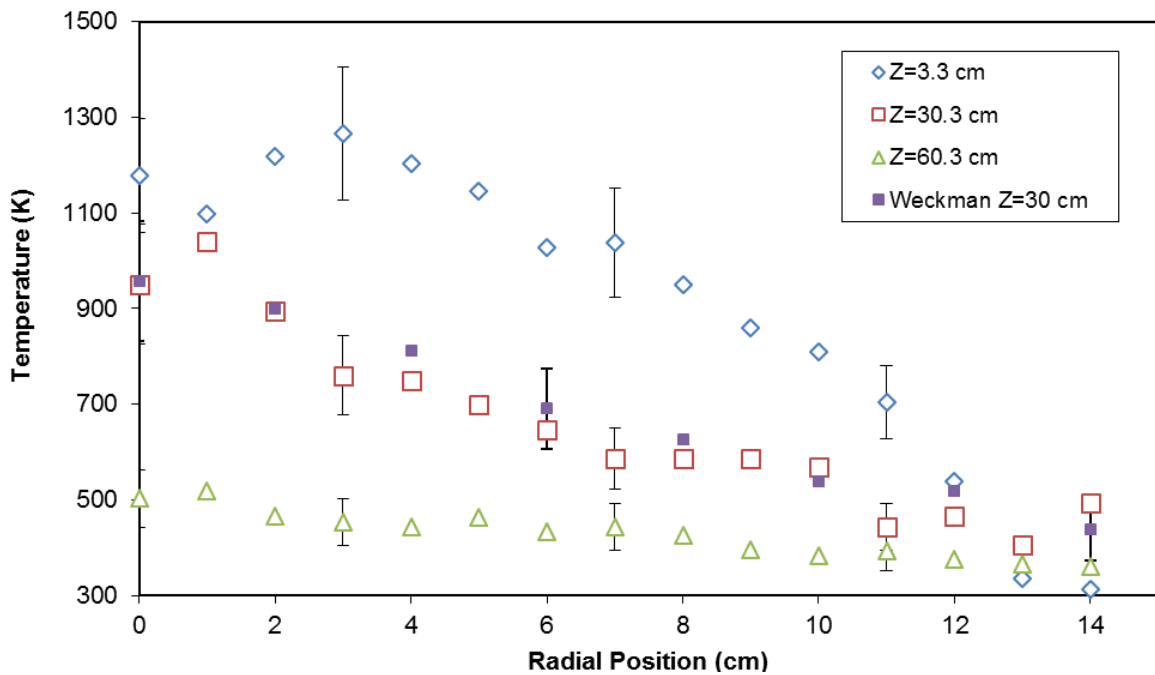


Figure 4. Fine wire radiation corrected thermocouple temperature profiles as a function of radial position at various axial distances above the burner in a 0.30 methanol pool fire. Results from Weckman and Strong are also shown [5].

### 3.2 Species Concentrations

Figure 5 shows a plot of the major species volume fraction along the central axis as a function of location above the burner rim, including the reactants ( $O_2$  and  $CH_3OH$ ), products ( $CO_2$  and  $H_2O$ ) and combustion intermediates ( $H_2$  and  $CO$ ). As expected, the fuel volume fraction is highest and the oxygen volume fraction is lowest close to the fuel surface. The intermediates peak a few cm above the fuel surface followed by the products that peak further downstream. This is seen more clearly in Figure 6, where the ratios of various gas species are presented. The expanded uncertainty was 48 % for the data points with measurement variance the dominant contributor to the uncertainty. The volume fraction ratios of  $H_2$  to  $H_2O$  and  $CO$  to  $CO_2$  are seen to decrease with distance from the fuel surface. Near the fuel surface, the  $CO$  volume fraction is greater than  $CO_2$  and remains so until about 0.1 m above the fuel surface. Figure 6 also shows that the ratio of carbon to oxygen atoms also decreases with distance from the fuel surface as more and more air is entrained towards the fire centerline.

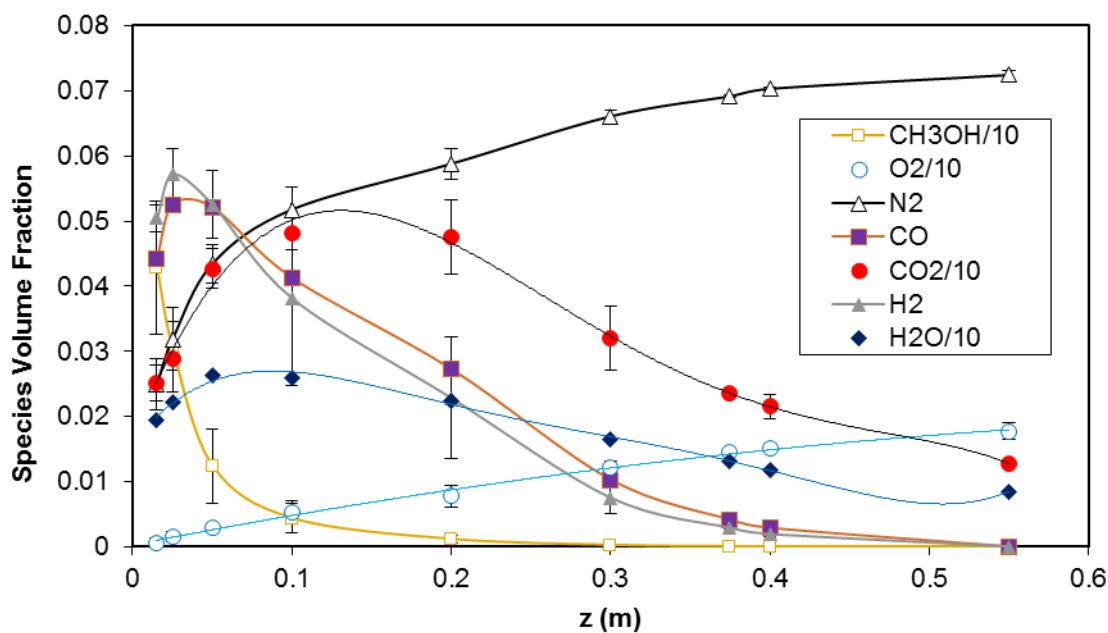


Figure 5. The volume fraction of major gas species as a function of distance ( $z$ ) above the burner along the centerline of a 0.30 methanol pool fire. The lines represent polynomial fits to the data.

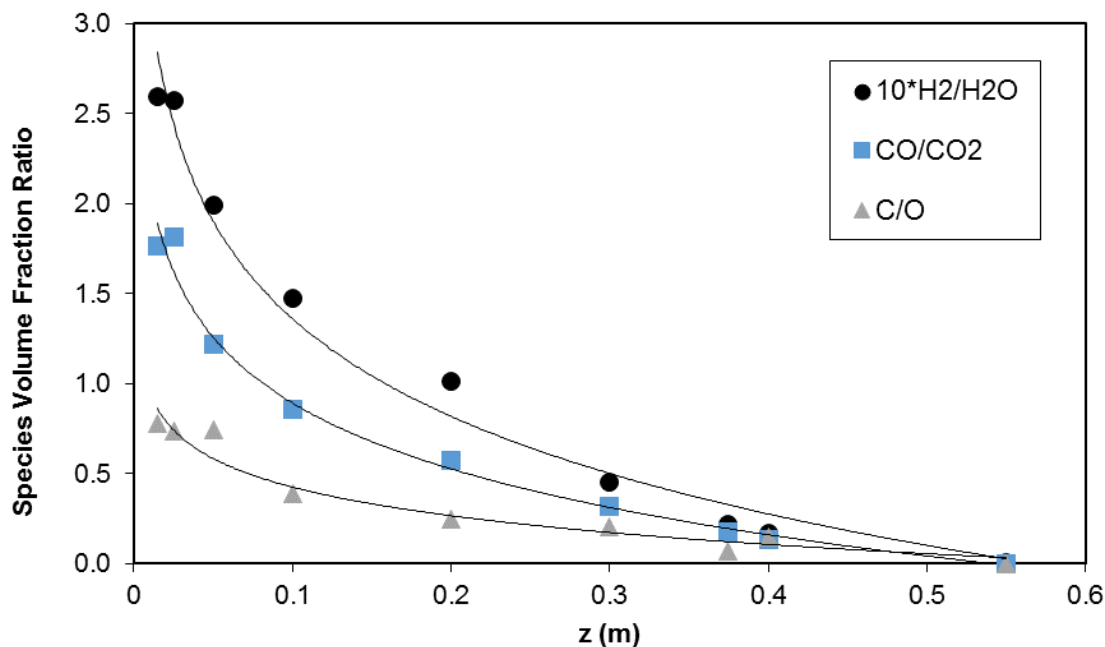


Figure 6. The ratios of the gas species volume fractions H<sub>2</sub> to H<sub>2</sub>O and CO to CO<sub>2</sub>, and the ratio of carbon to oxygen atoms as a function of distance (z) above the burner along the centerline of a 0.30 methanol pool fire. The expanded uncertainty was 48 %. The lines represent polynomial fits to the data.

### 3.3 Radiative Distribution

Figure 7 shows previously published results of the local heat flux in the downward direction within the pool and external to the pool along the plane defined by the burner rim as a function of radial position in the 30 cm methanol pool fire. The burner radius at 15 cm is noted in the figure. These data are taken from two independent studies using the same burner and conditions considered in this study [4, 6]. These measurements are useful to compare side-by-side to provide a more complete understanding of the structure of the methanol pool fire considered here.

The radiative flux within the pool was measured using a nitrogen-purged narrow view angle flux gauge positioned at various locations within the liquid pool [4]. The measurements required changing the angle of the radiometer and integrating the measurements to determine the total radiative flux at a specific location. Also shown are the local radiative heat flux measurements made along a radius external to the burner [6]. Axisymmetry of the pool fire was assumed in the processing of both these sets of measurements. The expanded uncertainty is shown in the figure. It is interesting to note the flux near the burner edge (15 cm) from these two set of measurements, which are in agreement within measurement uncertainty. This data along with previous measurements in this fire begin to provide a picture of the structure of this methanol pool fire.

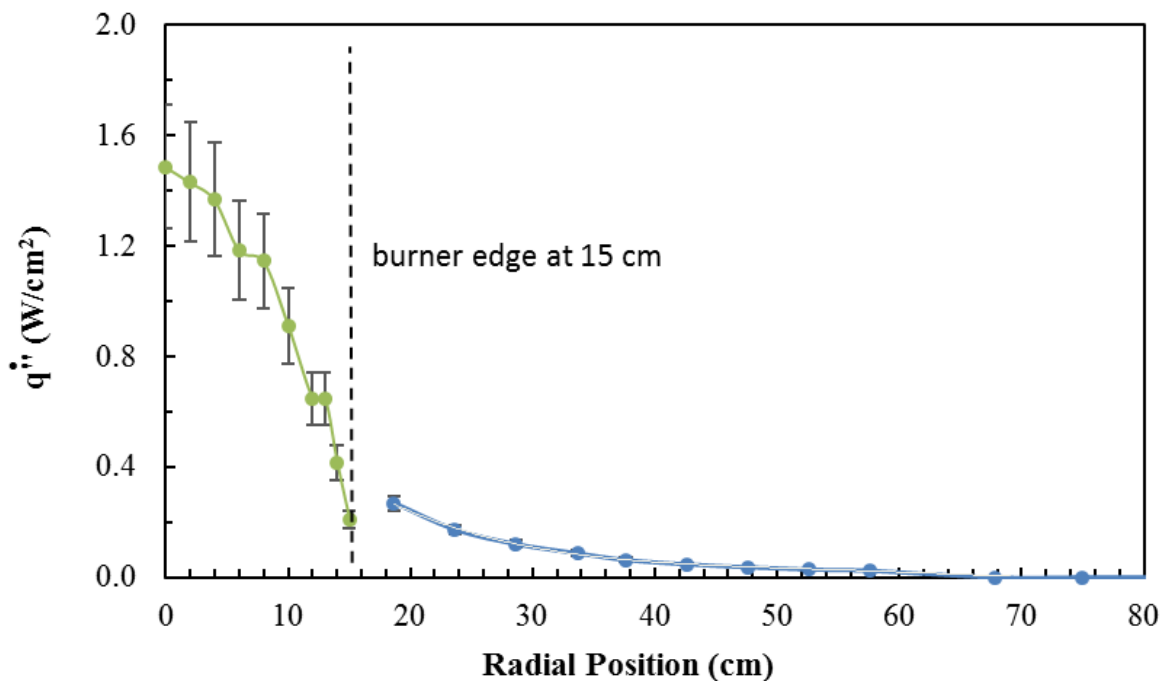


Figure 7. Local heat flux in the downward axial direction as a function of radial position at the plane defined by the burner rim in the 30 cm methanol pool fire. Data taken from Refs. [4, 6].

#### 4. CONCLUSIONS

In summary, a series of measurements was conducted to characterize the structure of a 30 cm diameter well-ventilated methanol pool fire burning in a quiescent environment. Time averaged local measurements of temperature and gas species concentrations were made. The measurements reported here complement previously reported data in the fire as noted in Table 1, such as the radiative distribution of heat flux, the flame height, the velocity field and so on. This accumulated information provides the basis for understanding the structure of the methanol pool fire and makes it a suitable candidate for fire model evaluation.

## 5. REFERENCES

1. Peacock, R.D., Reneke, P.A., Forney, G.P., CFAST – Consolidated Model of Fire Growth and Smoke Transport (Version 6), NIST Special Publication 1041r1, March 2013.  
<http://dx.doi.org/10.6028/NIST.SP.1041r1>
2. McGrattan, K., McDermott, R., Hostikka, S., Floyd, J., Weinschenk, C., Overholt, K., Fire Dynamics Simulator, NIST Special Publication 1019, Sixth Edition, April 2016.  
<http://dx.doi.org/10.6028/NIST.SP.1019>
3. Akita, K. and Yumoto, T., Heat Transfer in Small Pools and Rates of Burning in Liquid Methanol, Proceedings of the 10th Symposium of the Combustion Institute, 943-948 (1965).
4. Hamins, A., Klassen, M., Gore, J., Fischer, S., and Kashiwagi, T., Heat Feedback to the Fuel Surface in Pool Fires, *Combust. Sci. Tech.*, **97**, 37-62 (1993).
5. Weckman, E.J., and Strong, A.B., Experimental investigation of the turbulence structure of medium-scale methanol pool fires, *Combustion and Flame*, 105: 245-66 (1996).
6. M. Klassen and J.P. Gore, Structure and Radiation Properties of Pool Fires, *NIST Report GCR-94-651*, National Institute of Standards and Technology, Gaithersburg, MD, June 1994.
7. Hamins, A., Klassen, M., Gore, J., and Kashiwagi, T., Estimate of Flame Radiance via a Single Location Measurement in Liquid Pool Fires, *Combustion and Flame*, 86:223-228 (1991).
8. Hostikka, S, McGrattan, K., and Hamins, A., Numerical Modeling of Small and Moderate-Scale Pool Flames using Large Eddy Simulation and Finite Volume Method for Radiation, *Proceedings Seventh Int. Sym. on Fire Safety Science*, 383-394 (2003).
9. Klassen, M., Gore, J., Hamins, A., and Kashiwagi, T., Radiative Heat Feedback in a Toluene Pool Fire, *Proceedings Twenty-Fourth Sym. (Int.) on Combustion*, The Combustion Institute, 1713-1719 (1992).
10. Yilmaz, A., Radiation Transport Measurements in Methanol Pool Fires with Fourier Transform Infrared Spectroscopy, NIST Grant/Contractor Report GCR 09-922, January 2009.
11. Hamins, A., Kashiwagi, T., and Buch, R., Characteristics of Pool Fire Burning, in *Fire Resistance of Industrial Fluids, ASTM STP 1284* (Eds: G. Totten and J. Reichel), American Society for Testing and Materials (ASTM) Publication Number 04-012840-12, W. Conshocken, PA, pp. 15-41 (1995).
12. Incropera, F.P., DeWitt, D.P., Bergman, T.L., Lavine, A.S., Fundamentals of Heat Transfer, 6th ed., Wiley, 2007.
13. Lock, A., Bundy, M., Johnsson, E.L., Hamins, A., Ko, G.K., Hwang, C., Fuss, P., Harris, R., *Experimental Study of the Effects of Fuel Type, Fuel Distribution, and Vent Size on Full-Scale Underventilated Compartment Fires in an ISO 9705 Room*, NIST Technical Note 1603, National Institute of Standards and Technology, Gaithersburg, MD, October 2008.
14. Weckman, E.J., and Sobiesiak, A., The Oscillatory Behavior of Medium-Scale Pool Fires, *Proceedings of the Twenty-Second Sym. (Int.) on Combustion*, The Combustion Institute, 1299-1310 (1988).
15. Baum, H. R., and McCaffrey, B. J., Fire Induced Flow Field - Theory and Experiment, *Proceedings of the Second International Symposium on Fire Safety Science*, Hemisphere, New York, 129-148 (1989).